Photothermal Melting and Energy Migration in Conjugated Oligomer Films Doped with CdSe Quantum Dots

Artjay Javier, Robert W. Meulenberg, C. Steven Yun, and Geoffrey F. Strouse*

Department of Chemistry and Biochemistry, Florida State University, Tallahassee, Florida 32306-4390

Received: December 14, 2004; In Final Form: February 14, 2005

The effect of thin film morphology on energy transfer and migration in host−guest systems involving a phenylene−ethynylene oligomer matrix doped with colloidally prepared CdSe quantum dots is studied. Using correlated spectroscopy techniques including DSC, Raman, and temperature-dependent photoluminescence, we find that annealing the film produces continuous domain structures that enhance excitation migration by extending the excitation diffusion length. Under optical excitation, the thin films exhibit rapid melting of the host lattice, followed by resonant energy transfer to the CdSe QD guests. The ability to optically manipulate the structure and subsequently optically detect this change makes this material an important candidate for an all-optical read-write memory system.

I. Introduction

The combination of the rapid processability of conducting polymers[1−4] with the tunability of semiconductor quantum dots[5−7] makes the hybridization[8−10] of these two materials a potential candidate for device-oriented designs,[11−13] most notably electrooptical memory. Such unconventional design approaches can ideally lead to hybrid systems that benefit from the strengths of both materials, without suffering from the weaknesses of the precursors. The challenges in this field entail overcoming the strong electrical and optical induced charging[14,15] of the quantum dots, which reduces the quantum yield and therefore the overall performance of the material. Such a challenge can be overcome by employing alternate means of addressing and manipulating the quantum dot such as using resonant dipolar coupling.

In a previous publication[16] we explored the intimate interaction between a phenylene−ethynylene oligomer and CdSe quantum dots, wherein we were able to observe strong size-dependent electronic energy transfer that conferred a high degree of interaction between the two systems. The guiding principle in this system was that control of energetically resonant interactions are tunable through quantum dot size. The intimate conjugation between the two systems produced a rigidly bound monolith, whose optical characteristics remained extremely stable. In this manuscript, we report on the study of the unbound variant of this hybrid system, wherein thermodynamic transitions within the oligomeric domains becomes the primary factor for tuning the electronic properties.[17] This system involves a matrix of amorphous oligomer to which quantum dots have been doped in very small quantities (<1%). Bulk thermodynamic transitions from the oligomer matrix (energy transfer donor) are thus optically detected using the dopant (energy transfer acceptor) photoluminescance (PL). Specifically, the films are initially formed in a thermodynamically metastable phase or glassy state. Direct heating of the film in this amorphous metastable state melts the structure, which is followed by a nonreversible transition to a more thermodynamically stable, crystalline phase. The dopants introduced into this matrix do not affect the overall conformation but act only as optical reporters of the phase transition. Indirect heating by optical means can be achieved and is exploited for using this material in a read−write manner. This demonstration not only underscores the importance of this material as a new optical material but also highlights its potential use as a medium for optically addressable and readable memory.

Electronic energy transfer,[18,19] a nonradiative process where electronic energy is transferred from an electronically excited energy donor to an acceptor moiety, is a phenomenon found in condensed phase materials ranging from biological entities to doped semiconductor crystals.[20,21] In the latter case, typically the host matrix acts as the energy donor, and the dopant material acts as the energy acceptor. Optical or electrical excitation of the host material can result in efficient dopant photoluminescence as the host's pseudoparticles (excitons, phonons, etc.) act as conduits in the transfer of that energy. Though this case generally represents coherent energy transfer, it is important to recognize that in amorphous films, energy transfer still occurs via resonant energy migration[22] wherein the energy moves from domain to domain within the host in a random-walk pattern until it reaches the energy acceptor.[23] The rate of this energy diffusion will be strongly dependent on the general conformation and local domain interactions of the host material,[24] as well as the electronic energy topography.

Quantum confinement produces size-dependent electron and hole energy levels for CdSe in a size regime between ∼1 and 10 nm. The resulting size-dependent trend in the exciton energy provides a remarkable tunability for this material to be exploited in both applied and pure science endeavors. In particular, CdSe can be employed both as an energy trap[25] for the migrating excitation in a host−guest system and as an optical reporter for when the excitation has arrived at the CdSe quantum dot. Were this material to undergo a structural phase transition, the energy diffusion rate would be strongly affected and therefore the dopant photoluminescence may be strongly enhanced or quenched. This suggests tracking changes in energy transfer through a reporter entity can provide insight into changes in the host lattice conformation. Although a significant number of studies have been performed using CdSe as the dopant in conjugated polymer matrixes, to the authors' knowledge, this

* Corresponding author. E-mail: strouse@chem.fsu.edu.

10.1021/jp044303h CCC: $30.25
Published on Web 03/22/2005

manuscript reports the first attempt at the use of CdSe QDs as dopants in an oligomer matrix.

Although polyphenylene−ethynylene (PPE) and polyphenylene−vinylene (PPV) systems have been well-characterized,[1,26] significantly less is known about their oligomeric[27] variants, OPE and OPV. In particular, both theoretical and experimental studies have indicated that the photophysics of conjugated polymers change drastically in the limit of low repeat units, namely oligomers.[28,29] These short conjugated systems represent the crossover regime between solid-state phenomena[30] and molecular-like excited states. In fact, exciton lengths are not reached until roughly 30 Å (in the region of more than 5−8 repeat units)[31] in the oligomeric assemblies. In addition, due to the low repeat units, intrachain transport[32] (parallel to the long axis) is not as dominant and interchain energy migration (perpendicular to the long axis) can be strongly favored in these systems. For example, in anthracene matrixes, energy migration proceeds by inter-ring transfer with triplet exciton diffusion lengths exceeding 10 μm.[33] Ordered PPE films[24] have shown diffusion lengths of up to 10 nm. Thermodynamically, because each oligomer has only a few repeat units, their solid-state phases are much less thermodynamically stable than their polymeric counterparts owing to fewer interchain interactions (co-facial ring stacking and side chain associations) that confer stability.[32,34,35] This produces a competition between kinetically favored and thermodynamically favored solid-state phases, wherein kinetically favored but thermodynamically metastable glass states can easily form during the process of film deposition.

This paper is organized as follows: (1) We discuss phase transitions in the oligo-*p*-phenylene−ethynylene dibenzylthioacetate (OPE-1p) matrix, (2) we show how the optical properties arise from the morphology of the OPE-1p film, (3) we show how the film morphology can be optically manipulated, and (4) we show how CdSe QDs efficiently report these domain changes and how it can be used for read−write optical memmory.

II. Experimental Details

Synthesis. OPE-1p was prepared and purified as described in our previous report.[16] CdSe was prepared with an organic overcoating of HDA (hexadecylamine) as reported previously.[5]

Thin Film Preparation. Solid thin films were prepared in two ways. dc-Films were made by drop-casting concentrated solutions (~1 μM) of OPE-1 and/or CdSe QDs in toluene onto sapphire flats and allowed to dry on top of a warm oven (~10 0.1 mm). sc-Films were made by spin-casting dilute solutions (~1 nM) of OPE-1 and/or CdSe QDs in toluene at slow spinning speeds (~10 monolayers). Doped thin films were prepared in both methods by careful preparation (using microliter syringes) of mixed OPE-1p/CdSe solutions made from stock solutions. In both cases, film thickness was kept optically dilute and transparent (<0.1 absorbance at λ_{exc}).

Differential Scanning Calorimetry. DSC was performed on 10−12 mg of OPE-1p crystal or on concentrated OPE-1/toluene solutions that were thickly deposited onto the sample pan by drop-casting. Several runs were performed at a ramping speed of 10 °C/min, and reversibility was tested by repeated cycling.

UV−Vis Spectroscopy. Absorbance spectroscopy was performed using a Varian Instruments UV−vis spectrometer at room temperature in 1 cm quartz cells for solutions and sapphire flats for thin films. The UV−vis spectra of doped films and standard solutions showed exclusively OPE-1 absorption, with an undetectable or negligible amount of CdSe present.

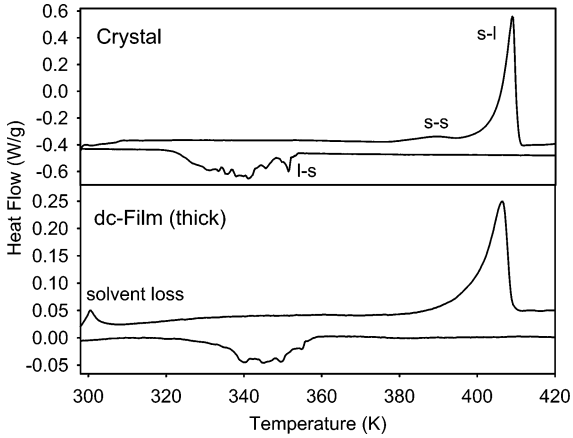

Figure 1. Differential scanning calorimetry data for OPE-1p in the drop-cast film form (bottom) and the single crystal form (top). Features are labeled to indicate the state−state transitions: s−l, solid-to-liquid; s−s, solid-to-solid; l−s, liquid-to-solid.

Raman Spectroscopy. Raman spectra were obtained by front-face sample excitation at 514 nm using an Ar^+ ion laser (Spectra Physics), collection by a f-1 lens and collimation into a $^1/_2$ m monochromator (Acton). Laser light rejection was achieved using a super-notch filter.

Photoluminescence Spectroscopy. Photoluminescence of solid films was taken using the excitation of either a HeCd laser (325 nm) or the filtered 312 nm line of a Hg-arc lamp. Samples were placed in a cryostat where a vacuum of 10^{-3} mmHg was applied. Heating was achieved resistively through a calibrated heating rod connected to copper rings surrounding the sapphire substrate, producing a temperature range between room temperature to 420 K (±5 K). In the temperature-dependent experiments, the film was allowed to thermally equilibriate in the dark for at least 10 min before being exposed to excitation light. Sample excitation was kept to 2 s maximum during these experiments to reduce any photoinduced heating.

Front-face excitation was used for the He−Cd system, but 45° rear excitation was used for the Hg arc lamp. The luminescence was collected using a f-1 lens, and collimated to a $^1/_3$ m CVI spectrometer (150 g/mm). Detection was achieved with an air-cooled SBIG CCD (512 px × 512 px).

III. Structural Characterization

Inspection of the melting behavior of the OPE-1p films suggest complex liquid-crytalline behavior dependent on the method of preparation (Figure 1). The sample-dependent calorimetry seems to arise from subtle packing differences. Such complexity is commonplace in materials that exhibit liquid-crystalline behavior. In the single crystal a strong first-order exotherm is observed at 405 K (23 J/g), corresponding to a solid-to-liquid (s−l) transition, as found in similar DSC studies on polymeric variants.[36] Just prior to this transition, a small first-order solid-to-solid (s−s) transition takes place at 380 K (5 J/g). The s−s transition indicates the presence of a glassy solid that is accessed before the transition to a completely liquid phase or most likely arises from the melting of the OPE-1p side-chains[37] inducing chain mobility prior to the onset of melting. The glassy solid is reminiscent of liquid-crystalline phase transition with the onset of ring mobility. As the material cools from the liquid phase, several small, discrete endothermic transitions (20 J/g) are observed at lower temperatures than the melt at 360 K. This behavior is reversible as the crystal is run through several heating and cooling cycles. The cooling behavior differs from what is observed in the polymeric variant, wherein

a broadened distribution is found as a result of a distribution of states.[36] In the oligomeric version, because there is a single molecular structure, the discrete transitions must arise from a kinetically controlled combination of discrete intramolecular (ring twisting) and intermolecular (ring−ring stacking, side-chain packing) interactions, rather than a purely thermodynamic process consistent with the observation of metastable-state formation. Comparison of the areas under the DSC curves reveal the process is reversible, just kinetically unfavorable.

The DSC scan of the amorphous drop-cast film (dc-Film) shows a solvent loss peak at 305 K, which corresponds to the boiling point of toluene, followed by an identical s−l transition (9 J/g), as observed in the crystalline form. However, the transition to the glassy solid is not observed distinctly in the amorphous film. The strong asymmetry of the s−l transition toward lower temperatures indicates the presence of a broadened s−s transition such that the s−s transition occurs over a wider temperature range than the crystal and cannot be distinguished from the s−l transition. This suggests that the more disordered nature of the glassy dc-film is a kinetically driven process. This is logical in light of the probability of a distribution of states arising from chain disorder in the drop-cast films. Numerical integration of the DSC data reveals that the l−s transition (5 J/g) accounts for 56% of the energy released in the s−l transition. The remaining 44% most likely arises from weak, broad, unresolved peaks.

Assuming that the l−s transitions between the crystal and film to be proportional to each other, the sum of the energy of the s−l and s−s transitions in the crystal accounts for the energy in the s−l transition of the film. Therefore, we can expect drop-cast films to be structurally different from the crystals because the s−s crystalline−glass solid (T_g) transition occurs at higher temperatures. The presence of a weak endothermic transition at 385 K in the single crystal that moves to higher temperature in the drop-cast film strongly suggests that packing effects play an important role in the thermodynamic phases of the material. The presence of a complicated exothermic transition that does not remotely resemble the corresponding endothermic transition (in both temperature and peak shape) indicates a very complicated cooling cycle that may involve changes in kinetically slow processes arising from local domains in the sample. An important point that we will return to later is that all of these transitions represent reversible macroscopic processes for the average structure, although this does not suggest microscopic reversibility for local domains.

IV. Optical Characterization

Consistent with the expectations from the complex calorimetry data, the PL of OPE-1p films is strongly preparation-dependent, and the initial stock solution concentration and casting method show dramatic changes, as shown in Figure 2. This is attributable to the change in population density of various aggregate states trapped by the glassy oligomer structure formed following film casting. In a previous publication,[16] we used concentration-dependent absorbance and photoluminescence to demonstrate the evolution of the OPE-1p molecules into dimer-like and aggregate configurations arising from strong $\pi-\pi$ stacking driving forces. In solution, both molecular and dimer PL can be observed, mediated by the self-association equilibrium. The monomer spectrum dominates Figure 2a. The dimer PL can be predicted from the concentration-dependent PL of OPE-1p solutions by spectral subtraction, as shown in Figure 2b. This dimer state is strongly red-shifted[38] from the OPE-1p molecular PL, indicating that the lowest energy excited state

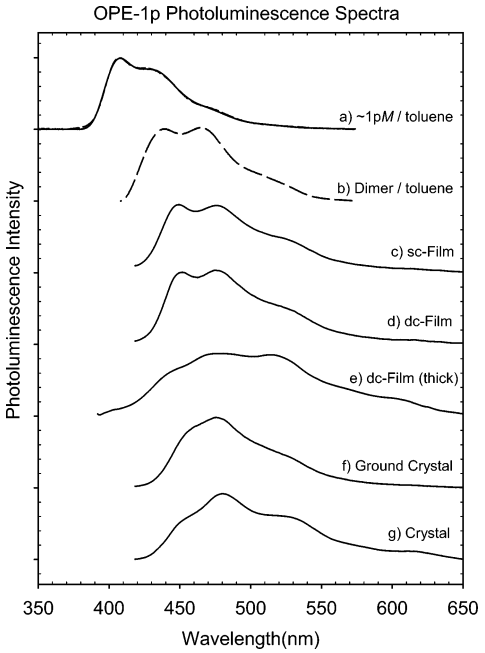

Figure 2. Photoluminescence spectra of OPE-1p cast under different conditions, all excited with 325 nm unpolarized light. (a) Dashed line for the OPE-1p/toluene solution at very dilute concentrations and solid line for the fit to eq 1 found in the Supporting Information. (b) Concentrated OPE-1p/toluene solution wherein the contribution from (a) has been spectrally subtracted. (c) Spun-cast film of OPE-1p using a low concentration stock solution. (d) Drop-cast film of OPE-1p using a low concentration stock solution. (e) Drop-cast film of OPE-1p using a high concentration stock. (f) OPE-1p crystals that have been coarsely ground with a mortar and pestle. (g) OPE-1p that crystallized a in chloroform solution.

from this interaction is dipole-allowed.[28] The vibronic separation in the OPE-1p dimer reveals an energy spacing of 1515 cm^{-1} that correlates with one of the observed vibrations obtained in the nonresonant Raman spectra (Supporting Information Figure 1) of the drop-cast film (1525 cm^{-1}).

When OPE-1p has been allowed to slowly crystallize (Figure 2g), the change in the ratio of the two bluest peaks changes dramatically, in addition to a very dramatic increase of the aggregate band at 620 nm. XRD data reveal $\pi-\pi$ stacking with rings with <7 Å separation, which gives rise to red-shifted aggregate PL,[39] as predicted by Bredas.[28−30] When the crystal is powdered with a mortar and pestle, again the PL spectrum changes dramatically (Figure 2f) and a change in the ratio of the two bluest transitions is observed, suggesting extreme sensitivity of the PL to the nature of the sample environment.

The spun-cast film (Figure 2c) shows a spectrum shaped similarly to the extracted solution-state dimer profile, though red-shifted due to changes in solvation. This suggests that much of the film PL structure arises from dimer-like states, making these the strongest emissive species within the films. In addition, due to the high probability for stacking in these molecules, an aggregate[27] band is observable at 620 nm that is related to excited states arising from association of more than two OPE-1p units. Drop-cast films (Figure 2d) produce similar spectra to the spun-cast counterparts, although the bluest peak appears to be slightly diminished.

Shown in Figure 2e is a film prepared by drop-casting a 1 M solution using several deposition steps, where we see a much broader PL profile that stretches across the entire visible spectrum and possesses peak features of OPE-1p molecules, dimers and aggregates. This casting method appears to produce the widest variation of domain structures, which gives rise to a

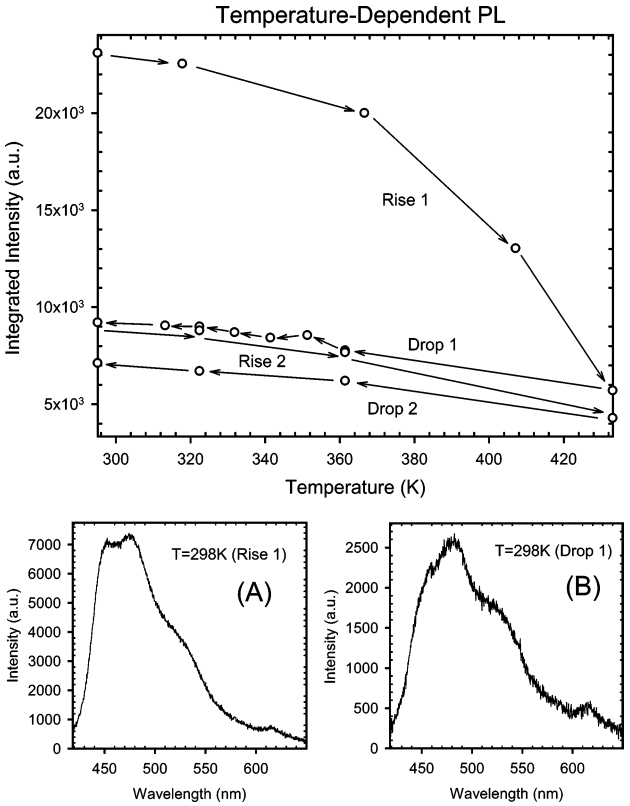

Figure 3. Spectrally integrated PL of OPE-1p drop-cast film as a function of applied temperature. The arrows indicate the direction of the heating cycle (rise 1,2) and cooling cycle (drop 1,2).

distribution of structures being probed by the laser and explains why the PL has elements of crystalline, amorphous, and isolated phases. Therefore, from the series shown in Figure 2, there is an overall trend in increasing PL shift to the red with decreasing OPE-1p intermolecular distances and more crystalline, tighter packed conformations.

The dependence of the PL intensity on the morphology offers a unique opportunity to probe the melting behavior of these oligomer structures. The temperature-dependent PL intensity on spun-cast films (Figure 3), can be correlated with the observed isotherms from the DSC (Figure 1). Trapped solvent loss ($T =$ 305 K) is trivial to the PL decay as no strong change in solvent loss occurs as the total PL drops by $<2\%$ as the solvent boiling point is surpassed. As the solid−liquid phase transition is reached ($T = 405$ K), the total integrated PL drops to 25%. During the cooling cycle, the integrated PL increases linearly with decreasing temperature, reaching 39% of the original value at room temperature. Therefore, the first heating/cooling cycle is not entirely reversible as the PL never recovers its original intensity. Although this is inconsistent with the observed reversibility of the DSC, it demonstrates the sensitivity of PL to probe local domains within the film, whereas DSC probes ensemble behavior.

As the film is cycled through repetitive heating−cooling ramps, the PL shows near reversibility as it tracks the cooling very closely. It reaches a slightly lower PL after the solid−liquid-phase transition ($\sim$21%). Subsequent cooling shows that the PL changes to $\sim$30% of its original intensity at room temperature. The irreversibility found in the second heating/cooling cycle ($<$10% PL change), however, is nowhere near as dramatic as that found in the first heating/cooling cycle ($>$75% PL change). This suggests a structural annealing process with increasing crystallinity due to removal of the metastable packing in the morphology of the cast film.

The shape of the PL spectrum provides a more systematic calibrant of the morphology changes. As a function of temperature, the PL switches between two forms as shown in Figure 3: (A) a high-temperature liquid form and (B) a low temperature solid form. The changes in the PL are distinctly observed to occur coincident with the transitions found in the DSC. Specifically, the initial metastable state of the OPE-1p film appears as (A) and there is no spectral change (apart from overall quenching) as the film is heated past the s−l phase transition. Even as the film cools initially, the spectral shape remains (A). However, as the endothermic transitions are surpassed during cooling, the spectra approach (B) until room temperature is reached. In subsequent heating to the s−l phase transition, the spectra remain as (B), but switch to (A) as the melting point is surpassed. Further cooling shows that (A) turns into (B) only as the endothermic cooling begins. The behavior is consistent with a kinetically trapped metastable conformation for the oligomers.

Examination of the temperature-dependent PL shows strong irreversibility after the first melting cycle, which contradicts the DSC where strong reversibility is observed over several heating and cooling cycles. Clearly, the PL reflects only a small population of emissive states. However, considering the dramatic change in the PL observed, the metastable state must have significantly higher quantum efficiency compared to the dimer state to account for the large disproportionality in population contribution. In polymeric variants it has been suggested that crystalline domains exhibit lower quantum efficiencies than more amorphous regions.[1,24,26]

V. Optical Manipulation

The effect of the initial OPE-1p concentration (density) on the final melted form can be examined by performing time-monitored laser PL on the drop-cast and spun-cast films. The drop-cast films are expected to have a higher density of OPE-1p and form into a more ordered state (crystalline aggregate domains) because of it, whereas the spun-cast films tend to be more amorphous and have a lower OPE-1p density. These results are shown in Figure 4. Here, we can see that over time under continuous irradiation, the PL intensity from the spun-cast films decays almost completely, within 2 h, whereas the PL from the drop-cast films decays to $\sim$50% of its original intensity and remains indefinitely stable at that intensity (inset of Figure 4). In addition, the spectral shape of the film PL initially resembles the liquid form of Figure 3A and then transforms into Figure 3B over time. Most notably, the 450 nm peak (molecule/dimer region) appears to quench more rapidly than the others (aggregate region).

The different PL behavior from the samples is examined more closely in Figure 5, where we have integrated the intensity over three different spectral regions that correspond to dimer PL (I,II) and aggregate PL (III). In the spun-cast film, we clearly see that the intensity of all three approach zero toward the end of the experiment. However, the dimer states (I,II) clearly decay at a very different rate from the aggregate state (III). In the drop-cast films, the dimer regions behave differently from each other with region I decaying to a lower overall PL than region II. In addition, region III does not decay below the initial intensity and in fact grows in intensity as regions I and II decrease in their intensity. In the dc-Film, all three regions appear to approach a stable intensity over the course of the experiment, which is in contrast to the spun-cast film where

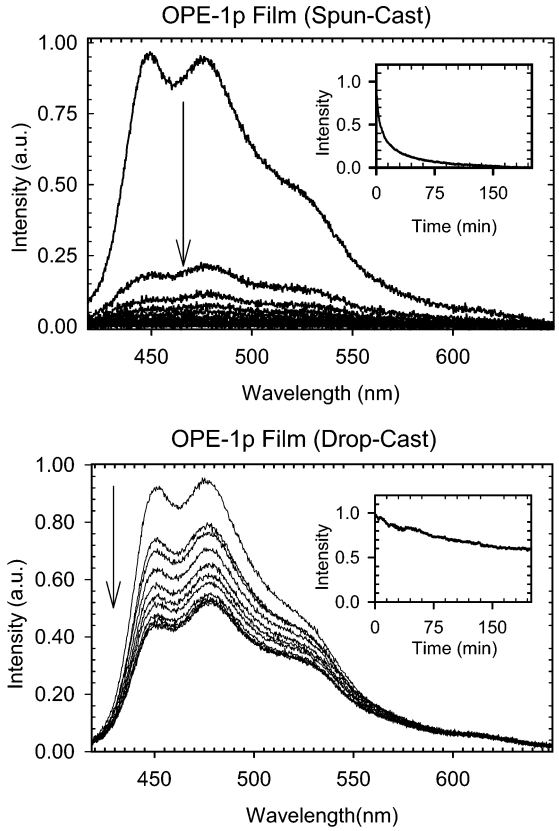

Figure 4. Photoluminescence spectra of OPE-1p films as a function of continuous irradiation time for spun-cast films (top) and drop-cast films (bottom). The curves (from top to bottom) represent spectra taken every 20 min after irradiation began. Insets show the integrated PL Intensity as a function of irradiation time.

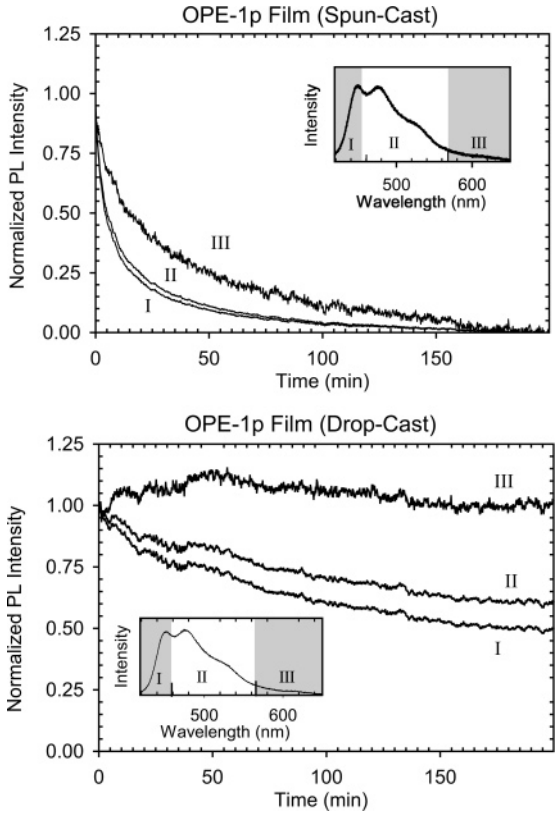

Figure 5. Spectrally integrated regions of the PL of OPE-1p films in 3 regions (I, II, III), shown in the insets, plotted against continuous irradiation time for both spun-cast (top) and drop-cast (bottom) films.

the intensity fades completely. All three regions in the drop-cast film also exhibit steplike increases in intensity at 5, 20, and 40 min. This phenomenon is also not present in the spun-cast film and could be due to discrete re-ordering of the structure that may correlate to the multiple kinetically trapped endothermic transitions observed in the DSC, suggestive of a glassy or liquid-crystalline-like ordering.

At a constant temperature (295 K), OPE-1p films display strong PL intensity and position instability, even in inert environments (Figure 5). To achieve this change in PL, there must be a corresponding change in the structure of the material, specifically, a transition from one thermodynamic phase to the other. This transformation is achieved by the dissipation of the absorbed optical energy through thermal deactivation processes. The heat released in this way eventually builds up and causes the local temperature to increase, eventually melting nearby chains. This process is very slow and strongly dependent on the applied laser power. The effect of this process on the stacking phenomenon can be seen in Figure 4. The spun-cast sample is much less dense and the heat applied through optical pumping induces the PL to degrade completely (Figure 5). This most likely occurs as a result of the wider separation between the OPE-1p domains. As the system absorbs heat, it begins melting, proceeding to the liquidlike phase. However, because the domains are spaced further apart, cooling into the thermodynamically favorable phase does not occur and the sample remains in the liquid phase. Because the PL signal appears to decay completely and very rapidly, the liquid phase must have very low quantum yield, very low optical cross section at the excitation wavelength, or both. The drop-cast film PL possesses very different characteristics. Although the film PL degrades, it does not degrade below 60% of its original intensity. In this case, the OPE-1p domains are spaced closely enough together that as the melting point is surpassed, cooling of the material proceeds into the thermodynamically stable phase, which is the final phase that the material will adopt when completely melted. In addition, if the PL spectra are spectrally analyzed over regions chosen to display primarily aggregate, dimer and monomer PL, as done in Figure 5, one can observe specific structural transformations occurring. In the drop-cast PL, while both monomer and dimer regions decay, the aggregate region increases in intensity, up to 120% of its original intensity. This represents an increase in the population of the aggregate phase, which is indicative of increased crystalline domains in the oligomer packing.

VI. Energy Transfer

The ability to tune optical properties in these films via laser irradiation suggests they may be practical for applications in optical memory via the influence on energy transport pathways. Excitation migration plays an important role in the PL properties of OPE-1p. Migration efficiency will be very different among each thermodynamic phase and will be strongly dependent on the size of the local domains. For example, migration can be strongly inhibited if the domain size is much smaller than the excitation diffusion length. Poorly formed films have a significant number of microscopic cracks that result in isolated islands of material, confining the migrating excitation. As heat is applied, the material melts and is allowed to cool, and the cracks are reduced, freeing the excitation to migrate between islands. In fact, because of the strong similarity of the initially formed OPE-1p films and both the liquified OPE-1p film and the solution-phase dimer, we can infer that the island sizes are small

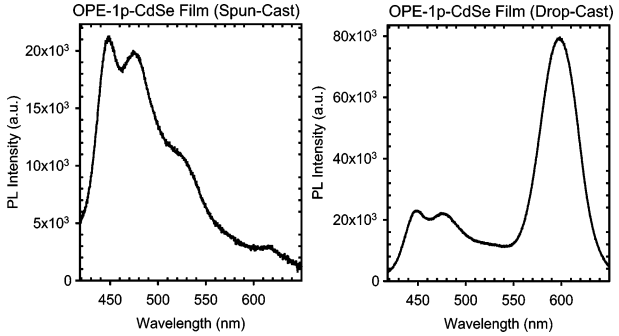

Figure 6. PL spectra of CdSe QD-doped OPE-1p films in spun-cast (left) and drop-cast (right) forms made from *identical* stock solutions, immediately after exposure to light.

enough that the dimer-PL experiences very little environmental (e.g., interdimer) influences.

The diffusion of an excitation in a 3D matrix of donors is a function of only four factors: D, the diffusion coefficient of the excitation; τ, the donor lifetime; $k_{EnT}(r - r_{DA})$, the energy transfer rate; and N_A, the number of acceptors in the matrix. The rate of movement of the probability density ($\rho(\vec{r},t)$) of an excitation in the case of 3D matrix of donors is[20]

$$\frac{\partial}{\partial t}\rho(\vec{r},t) = \left[D\nabla^2 - \frac{1}{\tau} - \sum_{j=1}^{N_A} k_{EnT}(|\vec{r} - \vec{r}_j|)\right]\rho(\vec{r},t) \quad (1)$$

From eq 1, we can see that migration is favorable as long as diffusion proceeds faster than the self-decay of the excitation. However, we also see that even in matrixes with large migration rates, and consequently distances, the effective migration rate can be reduced linearly by the number of dopant acceptors.

Now that we understand the physical, energetic and temporal evolution of the host lattice PL, we can be confident about accurately interpreting the QD-doped system where excitation migration plays a role. In this system, several important changes occur that ultimately lead to the determination of the fate of the excitation. An important aspect of host−guest systems is electronic communication between the host and guest, which can sometimes be manifested as migration of an electronic or optical species. Excitation migration can be resonant or non-resonant (phonon-coupled), and coherent or diffusive. In this system we expect the mechanism of migration to be largely resonant and diffusive, owing to the amorphous nature of the film.

Proof that a migration mechanism exists is given in Figure 6, wherein a CdSe−OPE1p film is prepared under two conditions. In the spun-cast form, only OPE-1p PL is seen due to the low density of film material. Here, excitation migration is inhibited as the large gaps between domains prevent the excitation from hopping from domain to domain. However, as the domains are brought closer together, as is representative of the drop-cast sample, excitation migration increases. This increase in excitation migration means that the energy of optically absorbed photons will eventually make it to the lowest energy trap centers in the material. One of these trap centers is the QD, which acts as an optical reporter for this phenomenon. As can be seen in the drop-cast film of Figure 6, this enhanced migration causes the CdSe to dominate the spectrum, nearly triple the intensity of the OPE-1p film.

Primarily, the character of the excitation will couple differently to CdSe in an energetically resonant sense, such that we can expect stronger energy transfer from more resonant states (like the dimer states). Due to the sensitivity of the metastable

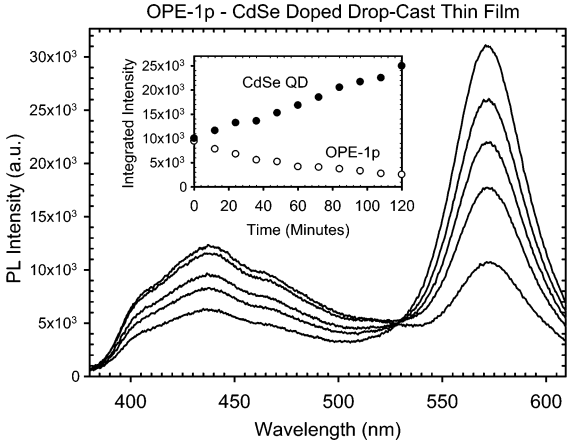

Figure 7. PL spectra of CdSe QD-doped OPE-1p drop-cast film as a function of irradiation time. The inset shows the integrated intensities in the region of OPE-1p PL and CdSe PL.

conformations to preparative means, we examine this system under different preparative protocols, in a spun-cast and in a drop-cast form, as shown in Figure 6. Because we will be using CdSe in very small concentrations in the doped films (<0.01%), it is safe to infer that *structurally* the OPE-1 system, which acts as the host, will largely behave as its undoped form. Colloidal additives are routinely added to plastics to improve properties without significant impact on the structure. Thus the primary effect of the CdSe QDs will be to act as structural probes, functioning *energetically* as excitation traps for the migrating electronic excitation in the film. This is the nanometer analogue to acceptor-doped semiconductor lattices, where the exciton localizes at these excitation traps, and strong PL is observed from them, i.e., acceptor luminescence.

In the spun-cast form, we observe only pure OPE-1p PL and there is no evidence that CdSe is even present as a dopant. However, we observe a strong combination of OPE-1p and CdSe PL in the drop-cast sample. Therefore, the PL that we observe must be a cooperative effect between the OPE-1p and CdSe, because it is only the casting method that determines the overall PL. This result also gives an example of the amount of PL from CdSe that results from direct excitation of CdSe. At such low dopant concentrations, it is not surprising to find that directly pumped CdSe PL is negligible. The difference in PL most likely results from differences in the film morphology and density. Although both systems are excited by excitation light, the drop-cast film allows for much better energy migration, which in turn allows for better energy transfer to the dopant and eventually higher acceptor PL.

Under continuous illumination, the PL of the drop-cast system will evolve to predominantly CdSe PL, as shown in Figure 7. The data shown in Figure 7 represent an experiment wherein the casting conditions and dopant concentrations were optimized to produce the most dramatic effect on the PL intensity. Here, a thick dc-film preparation has been used, analogous to Figure 2e, such that a distribution of monomers, dimers and aggregate conformations are formed. Here, we clearly see that thermally induced changes (through optical excitation) in the OPE-1p system strongly influence the energetic dynamics of the film PL. Over time, the OPE-1p PL will decay, while the CdSe PL will rise at the same rate. This shift from OPE-1p as the dominant emitting species to CdSe as the dominant emitting species is reflected in the isosbestic point observed at 530 nm.

An important application of this system is an all-optical information storage and retrieval technology, an "Optical Memory" system. As a prototype, we show how photothermal

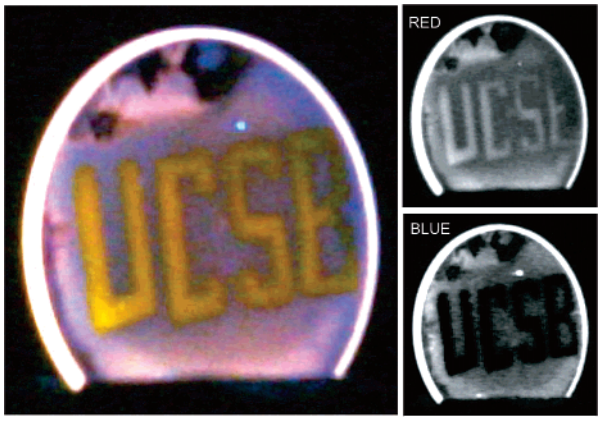

Figure 8. Digital photograph of a OPE-1p/CdSe sc-film illuminated with UV light from a Hg-lamp where an optical mask has been used to etch "UCSB" prior to photography. Color decomposition profiles for this image are shown on the right for red and blue channels.

melting of the OPE-1p matrix induces stronger energy transfer and migration to the CdSe QD, resulting eventually in increased CdSe PL (Figure 7). Therefore, we have used a laser to optically "write" into our film, producing a spectrum with enhanced PL from CdSe. This enhanced PL is then optically "read" by the monochromator/CCD we used, displaying an all-optical read-only memory system.

To demonstrate the feasibility of using this system, we show in Figure 8 how an OPE-1p film can be "written" using only an optical mask and the collimated UV light from a Hg lamp. After exposure to this light under a mask with the letters "UCSB" cut out, the mask was removed and a digital photograph of the film was immediately taken, while still under UV illumination. A RGB color decomposition was performed on the color image of Figure 8 and the red and blue color channels are shown on the right-hand side of Figure 8. Clearly, we can see from the blue channel that the OPE-1p PL (primarily blue-emitting) is not present in the regions of the lettering but is very visible in the regions surrounding it. In the red channel, where CdSe is the primary emissive species, the letters clearly form a readable positive image. Therefore in this demonstration we have shown that exposure of the OPE-1p/CdSe film to UV light results in primarily red light (from CdSe), the cause of which is directly linked to a photothermal melting and annealing of the OPE-1p domains resulting in more efficient energy migration and transfer to CdSe. As can be seen from Figure 8, using a crude writing method, millimeter resolution can be achieved. Collimated light from the mask is shrunken using a lens system and submillimeter writing resolutions were achieved, though they could not be easily photographed.

Several factors exist that control the writing speed and volatility of the memory system. These include film casting density, CdSe dopant concentration, optical laser excitation power and CdSe dopant size.

VII. Conclusion

In this manuscript we have described three important areas to oligomer−QD interactions: (1) the effects of structural phase transitions on the excited states of the OPE-1p film, (2) optically addressing and manipulating the film, and (3) using these hybrid films to control energy transfer and migration for the purposes of optical memory applications. The overall picture of the undoped OPE-1p film is that heating of the oligomer film induces a melting of the metastable film states and annealing to a more tighter, crystalline packing conformation. This is supported by a red shift in the overall PL, a distortion in the PL profile and a lowering of the quantum yield, all indicating the formation of electronically coupled states as well as the presence of energy migration through the matrix. As the CdSe dopants are added, the energy migrating within the matrix is funneled into the lower energy quantum dots and results in efficient QD PL. Because the annealing process is relatively slow, we can easily observe that the annealing process is coupled to the energy transfer process, and more importantly, the quantum dots act as the optical probes to this structural transformation.

We are currently undertaking the study of the excited-state decay dynamics of this system, in particular elucidating the primary participants in the energy transfer process. In addition, we are also undertaking more elaborate experiments for applying this technology to more nonvolatile memory systems (e.g., WORM, "Write Once Read Many") through control of laser power.

Acknowledgment. This work was supported by NSF-DMR 9875940. We thank G. Khitrov (UCSB) for preparation of some of the CdSe materials used.

Supporting Information Available: Raman spectra of the OPE-1p dimer is presented in Supporting Figure 1. In addition, the shift in the molecular vibrational frequencies with temperature are also shown. Spectral Fitting routines for the OPE-1p PL is described in the supporting information. This material is available free of charge via the Internet at http://pubs.acs.org.

References and Notes

(1) Deans, R.; Kim, J.; Machacek, M. R.; Swager, T. M. *J. Am. Chem. Soc.* **2000**, *122*, 8565.
(2) Nguyen, T.-Q.; Doan, V.; Schwartz, B. J. *J. Chem. Phys.* **1999**, *110*, 4068.
(3) Wang, P.; Collison, C.; Rothberg, L. *J. Photochem. Photobiol. A* **2001**, *144*, 63.
(4) Collison, C.; Treemaneekarn, V.; Oldham, W.; Hsu, J.; Rothberg, L. *Synth. Met.* **2001**, *119*, 515.
(5) Cumberland, S.; Hanif, K.; Javier, A.; Khitrov, G.; Strouse, G.; Woessner, S.; Yun, C. *Chem. Mater.* **2002**, *14*, 1576.
(6) Fogg, D.; Radzilowski, L.; Dabbousi, B.; Schrock, R.; Thomas, E.; Bawendi, M. *Macromolecules* **1997**, *30*, 8433.
(7) Yoffe, A. *Adv. Phys.* **2001**, *50*, 1.
(8) Wang, Y.; Herron, N. *J. Lumin.* **1996**, *70*, 48.
(9) Schmelz, O.; Mews, A.; Basche, T.; Herrmann, A.; Mullen, K. *Langmuir* **2001**, *17*, 2861.
(10) Sirota, M.; Minkin, E.; Lifshitz, E.; Hensel, V.; Lahav, M. *J. Phys. Chem. B* **2001**, *105*, 6792.
(11) Huynh, W. U.; Peng, X.; Alivisatos, A. P. *Adv. Mater.* **1999**, *11*, 923.
(12) Ginger, D.; Greenham, N. *Phys. Rev. B.* **1999**, *59*, 10622.
(13) Dabbousi, B.; Bawendi, M.; Onitsuka, O.; Rubner, M. *Appl. Phys. Lett.* **1995**, *66*, 1316.
(14) Javier, A.; Jennings, T.; Magana, D.; Strouse, G. F. *Appl. Phys. Lett.* **2003**, *83*, 1423.
(15) Javier, A.; Strouse, G. F. *Chem. Phys. Lett.* **2004**, *391*, 60.
(16) Javier, A.; Yun, C. S.; Sorena, J.; Strouse, G. F. *J. Phys. Chem. B* **2003**, *107*, 435.
(17) Javier, A.; Yun, C. S.; Strouse, G. F. *Mater. Res. Soc. Proc.* **2003**, *776*, 17.
(18) Agranovich, V.; Maradudin, A. *Electronic Excitation Energy Transfer in Condensed Matter*; Modern Problems in Condensed Matter Sciences; North-Holland Publishing Company: Amsterdam, 1982.
(19) Bernard, J.; Berry, D.; Williams, F. In *Energy Transfer Processes in Condensed Matter*; Bartolo, B. D., Ed.; Series B: Physics, Vol. 114; Plenum Press: New York, 1983; pp 1−102..
(20) Bartolo, B. D. In *Energy Transfer Processes in Condensed Matter*; Bartolo, B. D., Ed.; Series B: Physics, Vol. 114; Plenum Press: New York, 1983; pp 103−204.
(21) Klingshirn, C. In *Energy Transfer Processes in Condensed Matter*; Bartolo, B. D., Ed.; Series B: Physics, Vol. 114; Plenum Press: New York, 1983; pp 285−370.

(22) Herz, L.; Silva, C.; Phillips, R.; Setayesh, S.; Mullen, K. *Chem. Phys. Lett.* **2001**, *347*, 318.
(23) Brunner, K.; van Haare, J. A.; Langeveld-Voss, B. M.; Schoo, H. F.; Hofstraat, J. W.; van Dijken, A. *J. Phys. Chem. B* **2002**, *106*, 6834.
(24) Levitsky, I. A.; Kim, J.; Swager, T. M. *J. A. Chem. Soc.* **1999**, *121*, 1466.
(25) Kagan, C.; Murray, C.; Bawendi, M. *Phys. Rev. B* **1996**, *54*, 8633.
(26) Kim, J.; McHugh, S. K.; Swager, T. M. *Macromolecules* **1999**, *32*, 1500.
(27) Li, H.; Powell, D.; Hayashi, R. K.; West, R. *Macromolecules* **1998**, *31*, 52.
(28) Cornil, J.; dos Santos, D.; Crispin, X.; Silbey, R.; Bredas, J. *J. Am. Chem. Soc.* **1998**, *120*, 1289.
(29) Cornil, J.; Calbert, J.; Beljonne, D.; Silbey, R.; Bredas, J. *Synth. Met.* **2001**, *119*, 1.
(30) Shuai, Z.; Bredas, J. *Phys. Rev. B* **1995**, *52*, 13730.
(31) Knupfer, M.; Zojer, E.; Leising, G.; Fink, J. *Synth. Met.* **2001**, *119*, 499.
(32) Dellsperger, S.; Dotz, F.; Smith, P.; Weder, C. *Macromol. Chem. Phys.* **2000**, *201*, 192.
(33) Avakian, P.; Merrifield, R. *Phys. Rev. Lett.* **1964**, *13*, 541.
(34) Bunz, U. H.; Enkelmann, V.; Kloppenburg, L.; Jones, D.; Shimizu, K. D.; Caridge, J. B.; zur Loye, H.-C.; Lieser, G. *Chem. Mater.* **1999**, *11*, 1416.
(35) Egbe, D. A. M.; Roll, C. P.; Birckner, E.; Grummit, U.-W.; Stockmann, R.; Klemm, E. *Macromolecules* **2002**, *35*, 3825.
(36) Wautelet, P.; Moroni, M.; Oswald, L.; Moigne, J. L.; Pham, A.; Bigot, J. *Macromolecules* **1996**, *29*, 446.
(37) Ofer, D.; Swager, T. M.; Wrighton, M. S. *Chem. Mater.* **1995**, *7*, 418.
(38) Ding, L.; Egbe, D. A.; Karasz, F. *Macromolecules* **2004**, *37*, 6124.
(39) Yun, C. S.; Javier, A.; Strouse, G. Unpublished results.